



Investigation of surface properties of pristine and γ -irradiated PAN-based carbon fibers: Effects of fiber instinct structure and radiation medium

Liangsen Liu, Fan Wu, Hongwei Yao, Jie Shi, Lei Chen, Zhiwei Xu*, Hui Deng

Key Laboratory of Advanced Braided Composites, Ministry of Education, School of Textiles, Tianjin Polytechnic University, Tianjin 300387, PR China



ARTICLE INFO

Article history:

Received 15 January 2015
Received in revised form 13 February 2015
Accepted 13 February 2015
Available online 21 February 2015

Keywords:

Carbon fiber
Surface properties
 γ -Ray irradiation
Medium
Fiber instinct structure

ABSTRACT

The different rules for γ -ray modifications of carbon fiber (CF) surface were found in previous literature, and the contributing factors were not clear. To investigate the effects of fiber instinct structure and radiation medium on surface modification of CFs in γ -ray irradiation, argon atmosphere (Ar) and epoxy chloropropane (ECP) were chosen as the irradiation media for T300, T400, T700, T800 and T1000, respectively. Based on the Raman spectroscopy and specific surface area results, changes of surface graphitization and roughness depended on the fiber instinct structure after irradiation. The graphitization of T300, T400 and T800 with low graphitization and rough surface was increased after irradiation, while that of T700 and T1000 with high graphite degree and smooth surface was decreased. Specific surface areas of low-graphitization CFs (T300, T400 and T800) were changed clearly, while those of high-graphitization CFs (T700 and T1000) remained almost unchanged after irradiation. X-ray photoelectron spectroscopy provided the evidence that the surface chemistry change after irradiation was determined by the type of the irradiation medium. The oxygen ratio of CFs irradiated in Ar was decreased while that of CFs irradiated in ECP was increased with Cl element detected. Surface free energy of all CFs was improved obviously after irradiation, and CFs irradiated in ECP had higher surface free energy compared with CFs irradiated in Ar.

© 2015 Elsevier B.V. All rights reserved.

1. Introduction

Carbon fibers (CFs) have been widely used as reinforcing materials in composites because of their superior properties in strength, modulus, stiffness, lightness and resistance to elevated temperature [1,2]. It is widely accepted that the application of CFs is mainly dependent on the surface properties [3,4]. In order to improve the overall surface properties, various surface treatments have been carried out such as electrochemical processing [5,6], wet chemical oxidation [7,8], gas phase oxidation in ozone [9,10], high-energy beams (such as excimer laser beam [11], electron-beam [12]), plasma treatment [4,13], electrostatic spray painting [14], and so on. But almost all these methods have weakened the mechanical performance of CFs.

In recent years, it has been shown that γ -ray irradiation is an effective method for altering surface properties of CFs as well as other carbon materials [15–34], and can improve mechanical

performance of CFs to some extent. In the predecessors' works and our previous papers [19,20,24,35–39], modifications of polyacrylonitrile (PAN)-based CF surface induced by γ -ray irradiation were investigated exhaustively. It was convinced that both surface structure and surface chemistry were altered by γ -ray irradiation. It was found that the surface energy and amount of containing-oxygen functional groups were both increased significantly after irradiation [20–23,35,36,40,41]. Xu et al. [40] improved the surface energy of CFs from 42.2 mJ/m² to 50.5 mJ/m² after irradiation in acrylic acid. Li et al. [36] have modified the surface of CFs by γ -ray irradiation in air atmosphere, and found that the oxygen/carbon ratio of CF surface increased rapidly after irradiation.

However, there were some different opinions on the changes of surface roughness and degree of graphitization. Li et al. [20] investigated the structure and surface hydrophilicity of the CFs produced by Jilin Carbon Factory of China before and after γ -ray irradiation in air. There was no distinct surface morphologic change after irradiation and the graphitization degree determined by Raman was increased. In contrast to this, some researchers deemed that the surface roughness of PAN-based CFs was improved after irradiation [21,22,42] and the graphitization degree determined by Raman

* Corresponding author. Tel.: +86 022 83955231.
E-mail address: xuzhiwei@tjpu.edu.cn (Z. Xu).

was decreased [21,24]. For example, Xu et al. [40,43] have modified the surface of CFs which were manufactured by Institute of Coal Chemistry in epoxy resin and acrylic acid. It was found that degree of surface roughness was increased after irradiation with γ -rays. Presence of active medium or oxygen was considered as the reason for the increased oxygen/carbon ratio and surface roughness of CFs. Xiao et al. [24] studied the structure changes of T700 CFs which were produced by Toray after being irradiated in air. It could be observed that the degree of graphitization determined by Raman spectra was decreased and increased surface roughness was discovered.

As can be seen from the above results, there were different rules for changes of CF surface properties due to the difference in fiber instinct microstructure and radiation treatment process. Meanwhile, some researchers [24,40,43] have done some important work on the changes of CFs irradiated with different dose in air. It was found that surface properties were obviously changed at low irradiation dose, but the change trend with increasing dose was not similar to each other. It indicated that the instinct microstructure of CFs may play an important role in γ -irradiated modification of CFs. Today, a number of PAN-based CFs with different instinct structure (such as T300, T400, T700, T800 and T1000) have been commercially available, and can be used as the representative. Moreover, it was found that the media in γ -ray irradiation had significant influence on surface chemistry and morphology of graphene and carbon nanotubes [27–29]. Zhang et al. [27] demonstrated that graphene oxide appeared highly reduced and possessed high purity after γ -ray irradiation in alcohol and water in the absence of oxygen. While as reported in our previous work [59], graphite oxide was grafting and exfoliated after irradiated in different monomers by γ -rays. As for multi-wall carbon nanotubes (MWCNTs), Skakalova et al. [60] found that the effect of irradiation in air was much stronger in comparison to that in vacuum. While in our work, γ -ray irradiation decreased the inter-wall distance of MWCNTs and improved their graphitic order in air, while irradiation in ECP increased the inter-wall distance of MWCNTs and disordered the structure [61,62]. CF surface microstructure was similar to that of carbon nanotubes surrounded by multi-layer graphene sheets, and would be tailored by active or inert medium in γ -ray irradiation.

In this work, to understand the effects of fiber instinct structure and radiation medium on the surface properties of CFs in γ -ray irradiation, we conducted a systematic study of CFs irradiated in argon atmosphere (Ar) and epoxy chloropropane (ECP). After irradiation treatment, CFs were analyzed by Raman spectroscopy in order to investigate the effects of irradiation on their structure. Scanning electron microscopy (SEM) and specific surface area (SSA) were used to estimate the surface roughness of pristine as well as γ -ray irradiated CFs. X-ray photoelectron spectroscopy (XPS) and contact angles were used to estimate the surface chemistry and surface free energy of CFs.

2. Experimental

2.1. Pristine fibers

The PAN-based CFs were produced by Toray (Japan). The detailed information was presented in Table 1.

2.2. γ -Irradiation experiments

The five kinds of samples were placed in glass containers and irradiated in Ar and ECP at room temperature, respectively. Irradiation with ^{60}Co point-source irradiator was carried out at Tianjin Institute of Technical Physics. The absorbed dose was accumulated

Table 1
Physical properties of as-received PAN-based CFs.

	Tensile strength (MPa)	Tensile modulus (GPa)	Linear mass (g/km)	Density (g/cm ³)
T300	3530	230	198	1.76
T400	4410	250	396	1.8
T700	4900	230	800	1.8
T800	5490	294	445	1.81
T1000	6370	294	485	1.8

to 100 kGy with dose rate of 0.3 kGy/h, which was based on consulting previous literature [19,20,24,35–39].

2.3. Measurements

Raman spectroscopy was performed on a LABRAM-HR Confocal Laser Micro-Raman spectrometer using an Ar⁺ laser with 532 nm to determine the quality and graphitization of CFs before and after irradiation. The morphology of fibers irradiated in Ar and ECP was evaluated using a Hitachi S-4800 field-emission SEM system (operated at 4 kV). The SSA was calculated from the adsorption data in the relative pressure range between 0.05 and 0.35 using the Brunauer–Emmett–Teller (BET) method. XPS investigations were carried out with a PHI 5700 ESCA System with Al Ka (1486.6 eV) radiation to characterize changes of the chemical components of different CFs and the pressure in the XPS analyzing vacuum chamber was less than 3×10^{-9} mbar. The contact angles of various CFs irradiated were measured using the measurement instrument of dynamic contact angle (Dataphysics Co., Ltd.).

3. Results and discussion

3.1. Surface structure

Raman spectroscopy is often used to evaluate the degree of structural perturbation and stress/strain distribution. Note that the penetration depth of Raman measurements on the surface of CFs was estimated to be a few hundred angstroms [44,45] or 0.1–0.2 μm [46], which accounts for less than 5% of the fiber diameter. So Raman results only reflect the surface information of CFs. In the first order Raman spectra located at 1000–1800 cm⁻¹, CFs mainly show two characteristic bands. One is at around 1580 cm⁻¹, and denoted the G peak, corresponding to an ideal graphitic lattice vibration mode with E_{2g} symmetry, which is relative to the motion of sp² bonded carbon atoms [47,48]. Another Raman active band

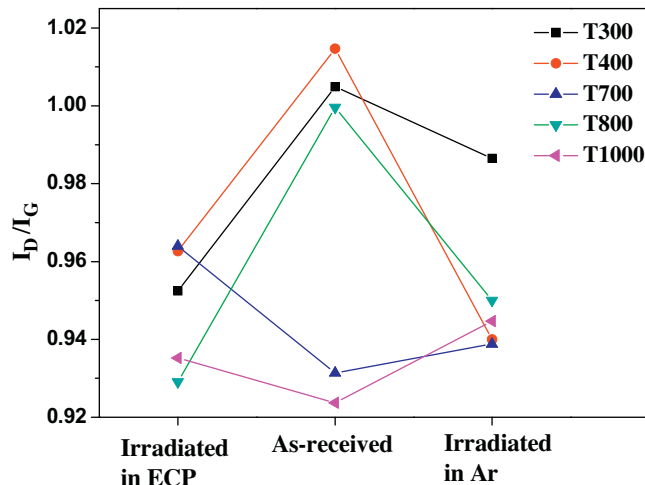


Fig. 1. $I_{\text{D}}/I_{\text{G}}$ of the CFs before and after irradiation in ECP and Ar.

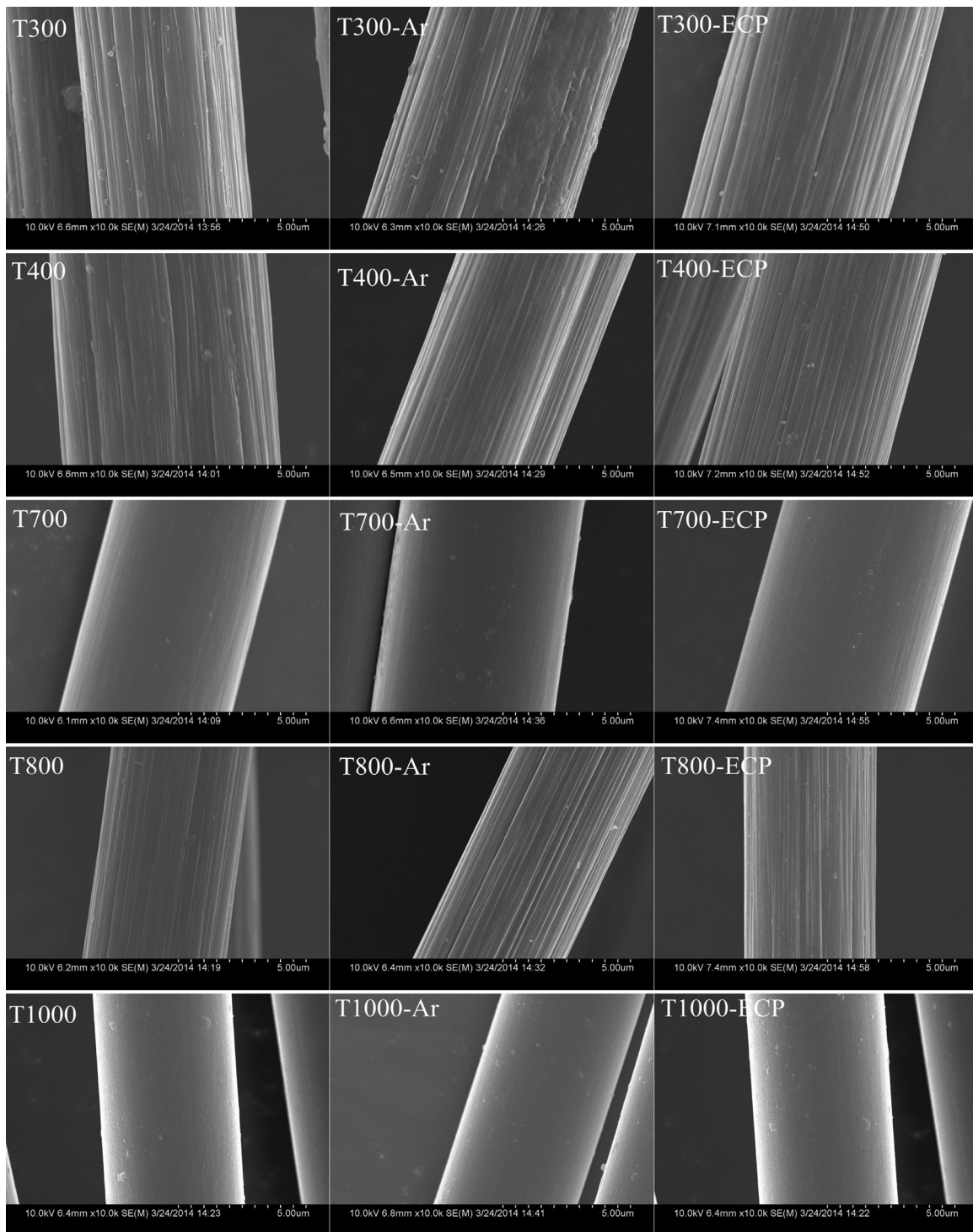


Fig. 2. SEM micrographs of pristine and irradiated fiber surface.

is the disorder-induced band at about 1360 cm^{-1} , called D band, which is associated with the concentration of bond defects (the bond defects could be considered as the carbon bands other than sp^2 bonds) in the structure and the intensity ratio of D and G, and $I_{\text{D}}/I_{\text{G}}$ can represent the relative change of bond defects of carbon materials [49,50]. $I_{\text{D}}/I_{\text{G}}$ ratio of CFs before and after irradiation was displayed in Fig. 1. The Raman spectra of pristine and irradiated CFs were supplied in Supplement. As shown in Fig. 1, the CFs were divided into two types clearly, T300, T400 and T800 with higher $I_{\text{D}}/I_{\text{G}}$ value which means low graphitization degree and T700 and T1000 with high graphitization degree.

The $I_{\text{D}}/I_{\text{G}}$ values of CFs irradiated in ECP and Ar were both increased (T700, T1000) or decreased (T300, T400 and T800) compared with original CFs. It indicated that the difference of irradiation medium did not influence the CF $I_{\text{D}}/I_{\text{G}}$ which reflected the changes in bond defect dynamics. The penetration depth of Raman measurement on CF surface was estimated to be a few hundred angstroms, which was much deeper than the affecting depth of the medium. So the medium was the inconclusive reason for the graphitization change of CFs.

The changes after γ -ray irradiation occurred because of Compton effect on fiber surface [20,24], which was affected by surface

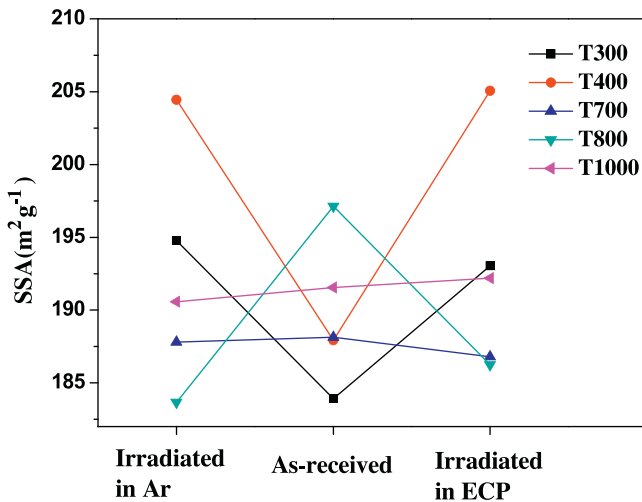


Fig. 3. SSA results of pristine and irradiated CFs.

graphitization of CFs. For low-graphitization CFs, the decrease of I_D/I_G after γ -ray irradiation indicated higher percentage of sp₂ hybridization carbon atoms and less disorder and defects in treated fibers, which was the evidence of the improvement of graphitization of the irradiated fibers [16]. The γ -induced atomic displacement was mainly responsible for the improvement of graphitization. It appeared that the energy transfer by recoiled electrons from Compton effect of γ photon to original defects accelerated their migration in CFs. Therefore, the defects including interstitials and vacancies were annealed via recombination of them.

While for high-graphitization CFs, there were seldom defects to be annealed. As shown in Fig. 1, the increased I_D/I_G values of high-graphitization CFs after irradiation indicated that many disordering carbon bonds were generated. The recoiled electrons from Compton effect were diverted from ordered graphene layers leading to abundant defects. Telling et al. [51] claimed theoretically that vacancy defects could be stabilized by forming complexes over the large interlayer distance, making cross-linking between neighboring graphene layers by means of creating pentagon-heptagon defects. According to the discussion of ref. [24], it was reasonable to assume that irradiation of CFs by high-energy γ -rays generated free radicals on the graphene layers and produced covalent cross-linking (bond defects) between the graphene layers of CFs.

3.2. Surface morphology

The surface topography of CFs irradiated in ECP and Ar was observed by SEM, and the results were shown in Fig. 2. Remarkable differences in morphology could be observed between low-graphitization CFs and high-graphitization CFs. It was clearly found that the surface of as-received high-graphitization CFs (T700 and T1000) was smooth, while the surface of as-received low-graphitization CFs (T300, T400 and T800) was rough. The PAN precursor and preparation process should be quite different among the above PAN-based CFs, which may be the main reason for the different surface topography of low-graphitization CFs and high-graphitization CFs. Compared with the similarly visible difference in surface morphology between irradiated low-graphitization CFs and high-graphitization CFs, there was no distinct surface morphologic change between the pristine and irradiated samples shown in Fig. 2. That may because the change of surface morphology could not be seen clearly. So the SSA results were taken to obtain the morphology after irradiation more accurately.

The SSA results were shown in Fig. 3. SSA results were calculated in the linear relative pressure range from 0.05 to 0.35 using the BET equation from acquired N_2 adsorption isotherms. There were two kinds of changes of SSA results shown in Fig. 3. For low-graphitization CFs, the SSA results changed after irradiation while the high-graphitization CFs did not show distinct difference after irradiation. The rough surface and low degree of graphitization of low-graphitization CFs were responsible for the obvious changes of SSA results. However, the SSA of T300 and T400 were increased, which indicated rougher surface after irradiation. It was opposite to T800 which had a decreased SSA after irradiation. The different instinct structure of T300, T400 and T800 may be responsible for the phenomenon [52,53]. T300 and T400 were produced by dry spinning, while T800 was produced by wet spinning. The difference in manufacturing technique was the main reason for the instinct structure difference among T300, T400 and T800. Because of dry spinning, T300 and T400 have some disordered grooves, while the grooves of T800 were more ordered than those of T300 and T400. The different contributing factor and morphology of surface groove may be the reasons for the different SSA changes of T300, T400 and T800 after irradiation. Similarly, no significant difference in surface morphology could be observed between CFs irradiated in ECP and Ar. It indicated that the medium was not the crucial reason for etching on the fiber surface.

3.3. Surface chemistry

XPS is a powerful method to characterize the surface chemical composition of both pristine and irradiated CFs. Wide scan spectra in the binding energy range 0–1350 eV were obtained to identify the surface elements present and carry out a quantitative analysis. The XPS spectra showed distinct carbon and oxygen peaks, representing the major constituents of the CFs investigated. The surface composition of pristine and irradiated CFs was determined by XPS and the results were given in Table 2. Carbon and oxygen were the major surface elements and small amounts of nitrogen amounting to less than 0.6% on the surface of pristine CF samples were detected. Cl element was found in CFs irradiated in ECP. It may be attributed to the grafting of monomers and the removal of weak surface layer on fiber surface.

As shown in Fig. 4, by analyzing the line shape of the C1s spectral envelopes of low-graphitization CFs and high-graphitization CFs before and after irradiation, it was possible to derive a rough sense of the functional groups present on the samples. For example, as shown in Fig. 4(a and e), T300 and T1000 after irradiation in ECP showed a spectral feature centered around 289 eV, indicative of photoelectrons from carbon atoms at the surface in highly oxidized environments (e.g. carboxyl or ester groups). There was also a distinct spectral feature centered around 286.8, which indicated the formation of carbonyl group [54]. Similar changes of other low-graphitization CFs and high-graphitization CFs were shown in Fig. 4(b–d). Overall, as displayed in Fig. 4 and Table 2, for both low-graphitization CFs and high-graphitization CFs after irradiation in ECP, more polar oxygen-containing functional groups were introduced onto fiber surface. However, the elements changes of low-graphitization CFs and high-graphitization CFs had different trend after irradiation in Ar. As shown in Fig. 4 and Table 2, lower oxygen ratio in CFs was found after being irradiated in Ar. The increase of carbon content of CFs after irradiation in Ar ranged from 2% to 3%. The amount of functional groups on fiber surface was responsible for tiny difference in carbon content increase of irradiated CFs.

Compton effect is mainly responsible for the above phenomenon [20]. γ Irradiation in solids causes ionization and chemical reactions due to radiolysis. When γ -quanta (photons) bombard the surface of CFs, Compton scattering may happen by means of originating the

Table 2

The element composition of pristine and irradiated CFs determined by XPS.

	As-received		Irradiated in ECP			Irradiated in Ar	
	C (%)	O (%)	C (%)	O (%)	Cl (%)	C (%)	O (%)
T300	86.99	13.01	85.88	13.47	0.65	88.95	11.05
T400	87.24	12.76	85.91	14.52	0.57	90.38	9.62
T700	89.27	10.73	83.67	15.65	0.68	91.95	8.05
T800	87.07	12.93	85.42	13.76	0.82	89.11	10.89
T1000	89.98	10.02	85.37	13.96	0.67	91.81	8.19

recoiled electrons with high kinetic energy. Carbon atom displacement would occur by these knock-on collisions. As the experiment was carried out in active medium, oxygen-containing functional groups were easily generated at chemically active dangling radicals via radiolysis. It should be noted that the penetrating depth of the laser beam in XPS tests is estimated to be about 6 nm, which accounts for less than 0.1% of the fiber diameter [55]. So the XPS results were sensitive to the changes of the surface.

Whereas the carbonization displayed in XPS results was responsible for the element changes of CFs when CFs were irradiated in Ar. Carbon atom on surface displaced when Compton scattering occurred on CFs. Since there was no other free radical species in

Ar, no functional groups were introduced onto the surface of the CFs. The functional groups on CF surface which were participants in Compton scattering were deoxygenized after irradiation. As a result, the fiber instinct structure leaded to very small changes in the element of irradiated CFs and the medium was the crucial factor for the changes of chemical composition on fiber surface.

3.4. Surface energy

To obtain the information about the surface activity of CFs before and after irradiation, an analysis of surface free energy was evaluated by dynamic contact angle analysis. The

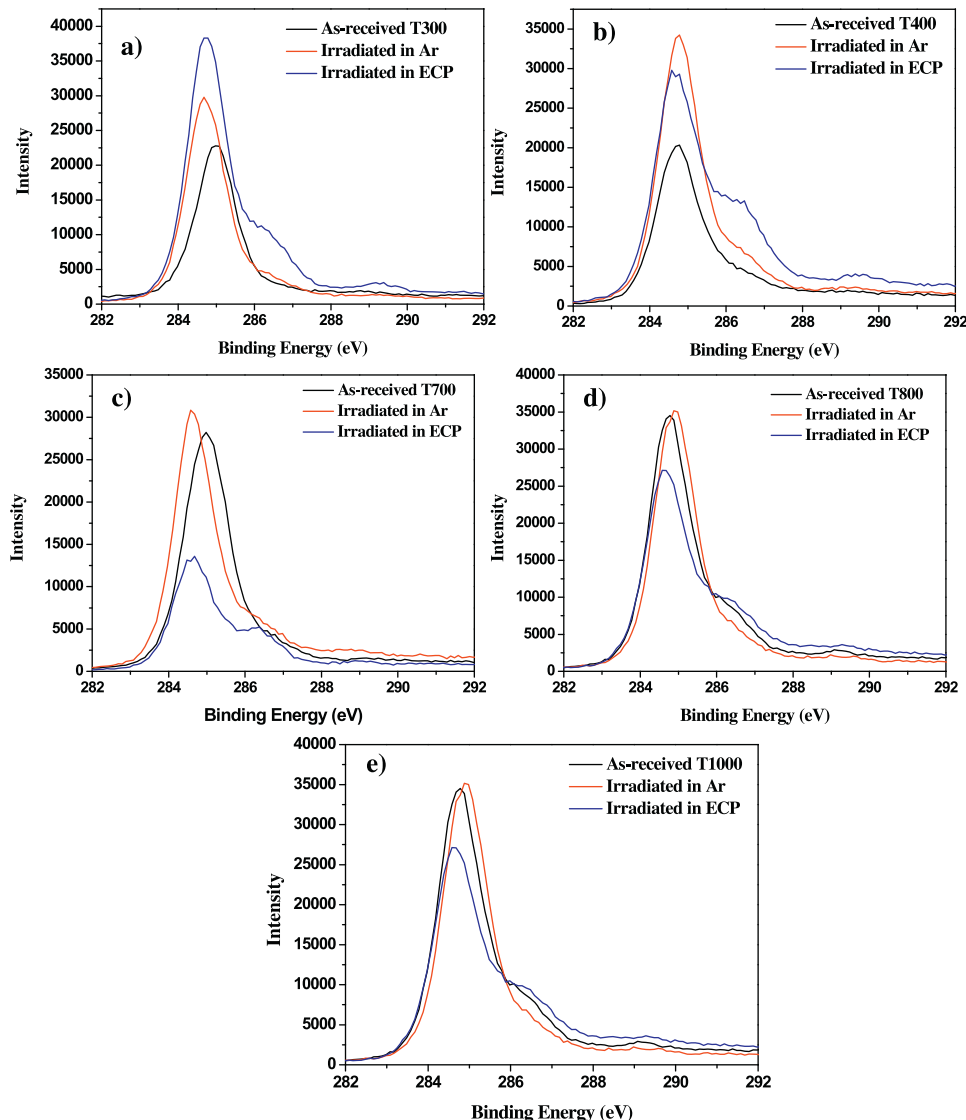


Fig. 4. (a–e) C 1s peak spectra of pristine and irradiated T300, T400, T700, T800 and T1000 determined by XPS.

Table 3

Contact angles and surface free energy of pristine and irradiated CFs.

		Contact angle with H ₂ O	Contact angle with CH ₂ I ₂	Polar component (mJ/m ²)	Dispersive component (mJ/m ²)	Surface energy (mJ/m ²)
T300	As-received	105.28	100.97	3.46	8.32	11.78
	Irradiated in Ar	83.71	100.11	13.93	8.63	22.56
	Irradiated in ECP	85.73	71.52	5.73	22.03	27.76
T400	As-received	66.96	87.05	6.38	14.04	20.42
	Irradiated in Ar	57.1	70.98	7.43	19.22	26.65
	Irradiated in ECP	85.54	54.59	3.22	31.68	34.90
T700	As-received	106.77	92.63	1.94	11.56	13.50
	Irradiated in Ar	81.37	98.1	14.89	9.37	24.26
	Irradiated in ECP	80.42	95.27	15.45	10.47	25.92
T800	As-received	86.24	102.41	12.96	12.06	21.28
	Irradiated in Ar	75.39	110.95	23.95	5.24	29.19
	Irradiated in ECP	75.67	143.85	35.1	0.47	35.57
T1000	As-received	55.09	79.67	7.34	17.66	24.00
	Irradiated in Ar	73.47	77.45	13.71	18.82	32.53
	Irradiated in ECP	69.78	76.44	15.82	19.35	35.17

double-liquid method was employed to determine the contact angle of CFs [51]. Here two various immersion liquids were used: deionized water and diiodomethane. The surface energy of deionized water is 72.8 mJ/m², where the polar and dispersive components are 50.7 and 22.1 mJ/m², respectively. The surface energy of diiodomethane is 50.8 mJ/m², where the polar and dispersive components are 0 and 50.8 mJ/m², respectively.

The surface energy of CFs can be determined by solving following equation.

$$\gamma(1 + \cos \theta) = 2\sqrt{\gamma_s^p \gamma^p} + 2\sqrt{\gamma_s^d \gamma^d} \quad (1)$$

$$\gamma_s = \gamma_s^p + \gamma_s^d \quad (2)$$

where γ , γ^d and γ^p represent the surface tension, dispersive component and polar component of immersion liquid, respectively. θ is the corresponding contact angle. γ_s , γ_s^d and γ_s^p represent the surface tension, dispersive component and polar component of CFs, respectively. Table 3 summarized the specific information of the CFs surface energy. It was clear that the surface energy of low-graphitization CFs and high-graphitization CFs were increased after irradiation. In addition, the CFs irradiated in ECP had higher surface energy than those irradiated in Ar basically.

The total fiber surface energy is the summation of the polar and dispersive energies, which means the polarity and roughness of CFs surface. The change of dispersive component shown in Table 3 was determined by the roughness of surface according to Eq. (1) [56]. In the case of low-graphitization CFs, the dispersive component changed distinctly after irradiation in Ar and ECP. While for high-graphitization CFs, there was no significant difference after irradiation. The results were in accordance with the results of BET.

Based on the above analysis, it could be concluded that exposure to γ irradiation caused significant surface energy changes on CFs despite of fiber instinct structure and irradiation medium. Moreover, there was a more remarkable increase in the surface energy of CFs irradiated in ECP, compared with that in Ar. The surface free energy indicated the wettability of CFs, which played a key role in the interfacial bonding between CFs and matrix [57,58]. The increasing surface free energy of all samples indicated that there may be a better composites interface for CFs after γ -ray irradiation.

4. Conclusions

To investigate the effects of fiber instinct structure and irradiation medium on surface modification of CFs in γ -ray irradiation,

T300, T400, T700, T800 and T1000 were irradiated by γ -rays in Ar and ECP. Major findings from this study were as follows:

- (1) Raman, SEM and BET analysis showed that T300, T400 and T800 showed similar surface graphitization and surface topography, and T700 and T1000 were considered to be members of a family. The graphitization of T300, T400 and T800 with low graphite degree and rough surface was increased after irradiation, while that of T700 and T1000 with high graphite degree and smooth surface was decreased. The SSAs of low-graphitization CFs (T300, T400 and T800) were changed clearly, while those of high-graphitization CFs (T700 and T1000) remained almost unchanged. It was indicated that changes of surface graphitization and roughness depended on the fiber instinct structure mainly, regardless of the type of media.
- (2) XPS demonstrated that the oxygen ratio of CFs irradiated in Ar was decreased while that of CFs irradiated in ECP was increased with Cl element detected. The surface chemistry changes of CFs after γ -ray irradiation were determined by the type of radiation media and were not affected by fiber instinct microstructure. CFs were deoxygenized in Ar while oxygenized in ECP after irradiation.
- (3) Based on the surface energy analysis, the surface activity of CFs was improved obviously after irradiation. The effect of fiber instinct structure on surface energy of irradiated CFs was negligible and ECP surpassed generally Ar in the surface activity increase of irradiated CFs.

Overall, it can be concluded that fiber instinct structure and irradiation medium which were both neglected in previous work had important and essential influence on the structure changes and property alternation of PAN-based CFs under γ -ray irradiation. There were different rules for the property change of different fibers after γ -ray irradiation, which could provide insights for understanding the different conclusion in previous work, and offered a new possibility to the radical alteration of CF properties in further low-cost use of γ rays.

Acknowledgments

The work was funded by the Petrochemical Joint Funds of National Natural Science Fund Committee – China National Petroleum Corporation (U1362108) and China Postdoctoral Science Foundation (2014T70217).

Appendix A. Supplementary data

Supplementary data associated with this article can be found, in the online version, at <http://dx.doi.org/10.1016/j.apusc.2015.02.101>.

References

- [1] N. Dilsiz, J.P. Wightman, Surface analysis of unsized and sized carbon fibers, *Carbon* 37 (1999) 1105–1114.
- [2] M. Desaejer, M.J. Reis, A.M. Botelho do Rego, J.D. Lopes da Silva, I. Verpoest, Surface characterization of poly(acrylonitrile) based intermediate modulus carbon fibres, *J. Mater. Sci.* 31 (1996) 6305–6315.
- [3] K. Jang-Kyo, M. Yiu-Wing, High strength, high fracture toughness fibre composites with interface control – a review, *Compos. Sci. Technol.* 41 (1991) 333–378.
- [4] N. Dilsiz, N.K. Erinc, E. Bayramli, G. Akovali, Surface energy and mechanical properties of plasma-modified carbon fibers, *Carbon* 33 (1995) 853–858.
- [5] Z.R. Yue, W. Jiang, L. Wang, S.D. Gardner, C.U. Pittman, Surface characterization of electrochemically oxidized carbon fibers, *Carbon* 37 (1999) 1785–1796.
- [6] L. Szazdi, J. Gulyas, B. Pukanszky, Surface characterization of electrochemically oxidized carbon fibers: surface properties and interfacial adhesion, *Compos. Interfaces* 9 (2002) 219–232.
- [7] F. Severini, L. Formaro, M. Pegoraro, L. Posca, Chemical modification of carbon fiber surfaces, *Carbon* 40 (2002) 735–741.
- [8] X. Bing, L. Yun, Chemical modification and surface reactions on carbon fibers studied by SERS, *J. Raman Spectrosc.* 37 (2006) 1423–1426.
- [9] X.L. Fu, W.M. Lu, D.D.L. Chung, Ozone treatment of carbon fiber for reinforcing cement, *Carbon* 36 (1998) 1337–1345.
- [10] X. Chen, M. Farber, Y.M. Gao, I. Kulaots, E.M. Suuberg, R.H. Hurt, Mechanisms of surfactant adsorption on non-polar, air-oxidized and ozone-treated carbon surfaces, *Carbon* 41 (2003) 1489–1500.
- [11] S.J. Ablett, P.E. Dyer, B.L. Tait, J.A. Barnes, Velocity measurements in polyetheretherketone-carbon fiber composite using excimer laser generated ultrasound, *Appl. Phys. Lett.* 59 (1991) 3236–3238.
- [12] L. Mao, Y.S. Wang, Z.J. Zang, S.S. Zhu, H.S. Zhang, H.H. Zhou, Amino-functionalization of carbon fibers through electron-beam irradiation technique, *J. Appl. Polym. Sci.* 131 (2014) 8.
- [13] M.A. Montes-Moran, A. Martinez-Alonso, J.M.D. Tascon, R.J. Young, Effects of plasma oxidation on the surface and interfacial properties of ultra-high modulus carbon fibres, *Compos. Part A: Appl. Sci. Manuf.* 32 (2001) 361–371.
- [14] M. Barletta, A. Gisario, Electrostatic spray painting of carbon fibre-reinforced epoxy composites, *Prog. Org. Coat.* 64 (2009) 339–349.
- [15] M. Miao, S.C. Hawkins, J.Y. Cai, T.R. Gengenbach, R. Knott, C.P. Huynh, Effect of gamma-irradiation on the mechanical properties of carbon nanotube yarns, *Carbon* 49 (2011) 4940–4947.
- [16] T. Fillete, H.D. Espinosa, Multi-scale mechanical improvement produced in carbon nanotube fibers by irradiation cross-linking, *Carbon* 56 (2013) 1–11.
- [17] I. Velo-Gala, J.J. López-Peña, M. Sánchez-Polo, J. Rivera-Utrilla, Surface modifications of activated carbon by gamma irradiation, *Carbon* 67 (2014) 236–249.
- [18] D. Tošić, Z. Marković, M. Dramišanac, I. Holclajtner Antunović, S. Jovanović, M. Milosavljević, Gamma ray assisted fabrication of fluorescent oligographene nanoribbons, *Mater. Res. Bull.* 47 (2012) 1996–2000.
- [19] F. Zhao, Y. Huang, Uniform modification of carbon fibers in high density fabric by γ -ray irradiation grafting, *Mater. Lett.* 65 (2011) 3351–3353.
- [20] B. Li, Y. Feng, G. Qian, J. Zhang, Z. Zhuang, X. Wang, The effect of gamma ray irradiation on PAN-based intermediate modulus carbon fibers, *J. Nucl. Mater.* 443 (2013) 26–31.
- [21] S. Tiwari, J. Bijwe, S. Panier, Gamma radiation treatment of carbon fabric to improve the fiber–matrix adhesion and tribo-performance of composites, *Wear* 271 (2011) 2184–2192.
- [22] A.A. Arkhipov, V.P. Korkhov, V.V. Pudnik, Y.P. Rodin, Changes in the structure and properties of carbon fibre plastics with polysulfone matrix under the action of gamma rays, *Mekh. Kompoz. Mater.* 6 (1992) 822–888.
- [23] J.Q. Li, Y.D. Huang, S.Y. Fu, L.H. Yang, H.T. Qu, G.S. Wu, Study on the surface performance of carbon fibres irradiated by gamma-ray under different irradiation dose, *Appl. Surf. Sci.* 256 (2010) 2000–2004.
- [24] H. Xiao, Y.G. Lu, M.H. Wang, X.Y. Qin, W.Z. Zhao, J. Luan, Effect of gamma-irradiation on the mechanical properties of polyacrylonitrile-based carbon fiber, *Carbon* 52 (2013) 427–439.
- [25] L. Chen, Z. Xu, J. Li, B. Zhou, M. Shan, Y. Li, Modifying graphite oxide nanostructures in various media by high-energy irradiation, *RSC Adv.* 4 (2014) 1025–1031.
- [26] B. Safabonab, A. Reyhani, A. Nozad Golikand, S.Z. Mortazavi, S. Mirshadi, M. Ghoranneviss, Improving the surface properties of multi-walled carbon nanotubes after irradiation with gamma rays, *Appl. Surf. Sci.* 258 (2011) 766–773.
- [27] B. Zhang, L. Li, Z. Wang, S. Xie, Y. Zhang, Y. Shen, Radiation induced reduction: an effective and clean route to synthesize functionalized graphene, *J. Mater. Chem.* 22 (2012) 7775.
- [28] M.X. Han, Z.Y. Ji, L.W. Shang, Y.P. Chen, H. Wang, X. Liu, gamma radiation caused graphene defects and increased carrier density, *Chin. Phys. B* 20 (2011) 122–125.
- [29] S.A. Vitusevich, V.A. Sydoruk, M.V. Petrychuk, B.A. Danilchenko, N. Klein, A. Offenhausser, Transport properties of single-walled carbon nanotube transistors after gamma radiation treatment, *J. Appl. Phys.* 107 (2010) 6.
- [30] S.P. Jovanovic, Z.M. Markovic, D.N. Kleut, N.Z. Romcevic, V.S. Trajkovic, M.D. Dramicanin, et al., A novel method for the functionalization of gamma-irradiated single wall carbon nanotubes with DNA, *Nanotechnology* 20 (2009) 7.
- [31] J.A. Fagan, N.J. Lin, R. Zeisler, A.R.H. Walker, Effects of gamma irradiation for sterilization on aqueous dispersions of length sorted carbon nanotubes, *Nano Res.* 4 (2011) 393–404.
- [32] H.B. Yu, X.Y. Mo, J. Peng, M.L. Zhai, J.Q. Lia, G.S. Wei, et al., Radiation-induced grafting of multi-walled carbon nanotubes in glycidyl methacrylate-maleic acid binary aqueous solution, *Radiat. Phys. Chem.* 77 (2008) 656–662.
- [33] C.H. Jung, D.K. Kim, J.H. Choi, Y.C. Nho, K. Shin, D.H. Suh, Shortening of multi-walled carbon nanotubes by gamma-irradiation in the presence of hydrogen peroxide, *Nucl. Instrum. Methods Phys. Res. Sect. B: Beam Interact. Mater. Atoms* 266 (2008) 3491–3494.
- [34] S. Gupta, Irradiation-induced structural modifications in multifunctional nanocarbons, in: *Symposium on Diamond Electronics – Fundamentals to Applications Held at the 2006 MRS Fall Meeting*, Materials Research Society, Boston, MA, 2006, pp. 235–241.
- [35] S. Tiwari, J. Bijwe, S. Panier, Polyetherimide composites with gamma irradiated carbon fabric: studies on abrasive wear, *Wear* 270 (2011) 688–694.
- [36] J.Q. Li, Y.D. Huang, Z.W. Xu, Z. Wang, High-energy radiation technique treat on the surface of carbon fiber, *Mater. Chem. Phys.* 94 (2005) 315–321.
- [37] Z.W. Xu, Y.D. Huang, C.H. Zhang, L. Liu, Y.H. Zhang, L. Wang, Effect of gamma-ray irradiation grafting on the carbon fibers and interfacial adhesion of epoxy composites, *Compos. Sci. Technol.* 67 (2007) 3261–3270.
- [38] Z.W. Xu, Y.D. Huang, C.Y. Min, L. Chen, Effect of gamma-ray radiation on the polyacrylonitrile based carbon fibers, *Radiat. Phys. Chem.* 79 (2010) 839–843.
- [39] Z. Xu, L. Chen, B. Zhou, Y. Li, B. Li, J. Niu, et al., Nano-structure and property transformations of carbon systems under γ -ray irradiation: a review, *RSC Adv.* 3 (2013) 10579–10597.
- [40] Z.W. Xu, L. Chen, Y.D. Huang, J.L. Li, X.Q. Wu, X.M. Li, et al., Wettability of carbon fibers modified by acrylic acid and interface properties of carbon fiber/epoxy, *Eur. Polym. J.* 44 (2008) 494–503.
- [41] Z.W. Xu, Y.D. Huang, C.Y. Min, L. Chen, L. Chen, Effect of gamma-ray radiation on the polyacrylonitrile based carbon fibers, *Radiat. Phys. Chem.* 79 (2010) 839–843.
- [42] Z.W. Xu, J.L. Li, X.Q. Wu, Y.D. Huang, L. Chen, G.I. Zhang, Effect of kidney-type and circular cross sections on carbon fiber surface and composite interface, *Compos. Part A: Appl. Sci. Manuf.* 39 (2008) 301–307.
- [43] Z. Xu, Y. Huang, C. Min, S. Chen, Effect of irradiation grafting epoxy on surface characteristics of carbon fibers and mechanical properties of composites, *J. Rare Earths* 24 (2006) 375–380.
- [44] C. Galiotis, N.B. Batchelder, Strain dependences of the first- and second-order Raman spectra of carbon fibres, *J. Mater. Sci. Lett.* 7 (1988) 3.
- [45] F.J. Liu, H.J. Wang, L.B. Xue, L.D. Fan, Z.P. Zhu, Effect of microstructure on the mechanical properties of PAN-based carbon fibers during high-temperature graphitization, *J. Mater. Sci.* 43 (2008) 4316–4322.
- [46] M.B. Vazquez-Santos, E. Geissler, K. Laszlo, J.N. Rouzaud, A. Martinez-Alonso, J.M.D. Tascon, Comparative XRD, Raman, and TEM study on graphitization of PBO-derived carbon fibers, *J. Phys. Chem. C* 116 (2012) 257–268.
- [47] J. Robertson, Diamond-like amorphous carbon, *Mater. Sci. Eng. R: Rep.* 37 (2002) 1–281.
- [48] H. Ching-Cheh, J. Miller, Thermal conductivity of pristine and brominated highly graphitized pitch based carbon fibers, *Carbon* 25 (1987) 679–684.
- [49] Z. Zafar, Z.H. Ni, X. Wu, Z.X. Shi, H.Y. Nan, J. Bai, et al., Evolution of Raman spectra in nitrogen doped graphene, *Carbon* 61 (2013) 57–62.
- [50] M. Hulman, V. Skakalova, S. Roth, H. Kuzmany, Raman spectroscopy of single-wall carbon nanotubes and graphite irradiated by gamma rays, *J. Appl. Phys.* 98 (2005) 5.
- [51] R.H. Telling, C.P. Ewels, A.A. El-Barbary, M.I. Heggie, Wigner defects bridge the graphite gap, *Nat. Mater.* 2 (2003) 333–337.
- [52] C. Wilms, G. Seide, T. Gries, Relationship between process technology, structure development, and fiber properties in modern carbon fiber production, *Abstr. Pap. Am. Chem. Soc.* 245 (2013) 1–5.
- [53] D. Zhang, Q. Sun, Structure and properties development during the conversion of polyethylene precursors to carbon fibers, *J. Appl. Polym. Sci.* 62 (1996) 367–373.
- [54] T.A. Langston, R.D. Granata, Influence of nitric acid treatment time on the mechanical and surface properties of high-strength carbon fibers, *J. Compos. Mater.* 48 (2013) 259–276.
- [55] H.J. Mathieu, Auger electron spectroscopy, in: *Surface Analysis – The Principal Techniques*, John Wiley & Sons Ltd., 2009, pp. 9–45.
- [56] F. Zhao, Y. Huang, L. Liu, Y. Bai, L. Xu, Formation of a carbon fiber/polyhedral oligomeric silsesquioxane/carbon nanotube hybrid reinforcement and its effect on the interfacial properties of carbon fiber/epoxy composites, *Carbon* 49 (2011) 2624–2632.
- [57] L. Peng, F. Yi-yu, Z. Peng, C. Hui-min, Z. Naiqin, F. Wei, Increasing the interfacial strength in carbon fiber/epoxy composites by controlling the orientation and length of carbon nanotubes grown on the fibers, *Carbon* 49 (2011) 4665–4673.
- [58] Q. Hui, A. Bismarck, E.S. Greenhalgh, G. Kalinka, M.S.P. Shaffer, Hierarchical composites reinforced with carbon nanotube grafted fibers: the potential assessed at the single fiber level, *Chem. Mater.* 20 (2008) 1862–1869.

- [59] L. Chen, Z.W. Xu, J.L. Li, et al., A facile strategy to prepare functionalized graphene via intercalation, grafting and self-exfoliation of graphite oxide, *J. Mater. Chem.* 22 (2012) 13460–13463.
- [60] V. Skakalova, A. Hulman, P. Fedorko, P. Lukac, S. Roth, Graphene: properties, preparation, characterisation and devices, in: *AIP Conf. Proc.*, vol. 685, 2003, pp. 143–147.
- [61] Z. Xu, L. Chen, L. Liu, X. Wu, L. Che, Structural changes in multi-walled carbon nanotubes caused by [gamma]-ray irradiation, *Carbon* 49 (2011) 350–351.
- [62] Z. Xu, C. Min, L. Chen, L. Liu, G. Chen, N. Wu, Modification of surface functionality and interlayer spacing of multi-walled carbon nanotubes using gamma-rays, *J. Appl. Phys.* 109 (2011) 543–553.